Numerical Study of Interaction Between Waves and Free Rolling Body by MPS Method

Youlin Zhang, Zhenyuan Tang, Decheng Wan*

State Key Laboratory of Ocean Engineering, School of Naval Architecture, Ocean and Civil Engineering, Shanghai Jiao Tong University, Collaborative Innovation Center for Advanced Ship and Deep-Sea Exploration, Shanghai 200240, China

*Corresponding author: dcwan@sjtu.edu.cn

Abstract

In the present study, an in-house particle solver MLParticle-SJTU based on improved Moving Particle Semi-Implicit (MPS) method is applied to numerically investigate the roll motions of a two-dimensional floating body in regular waves. Damped roll motion of a floating box is studied to validate effects of water viscosity and spatial resolution of particles. Then, Numerical Wave Tank (NWT) is developed, including wave making, wave absorb and six DOFs modules. Regular waves are simulated to study the accuracy of wave making, and wave elevation is in agreement with analytical solution. Finally, roll motions of floating body in waves with different frequencies are investigated, response amplitude operators (RAO) for roll motion are in good agreement with experimental data.

Keywords: Particle method; MPS (Moving Particle Semi-Implicit); Wave-body interaction; Wave making; Roll motion

Introduction

Due to increasing interest in the development of subsea resources, varies of floating structures are produced. Roll motions due to waves should be evaluated during designing a floating structure in naval, coastal and ocean engineering, because safety standards must be met.

Over the past few decades, numerical method is frequently employed to investigate the interaction between floating body and waves. Among these early established methods, potential-flow theories are most popular to solve the motion of floating body mounted in regular waves and with simple shape. The Mixed Eulerian-Lagrangian Boundary Element Method (BEM-MEL), introduced by (Longuet-Higgins and Cokelet, 1976), was used to simulate the motion of two-dimensional (2D) floating body, the effectiveness and accuracy was studied and also proved to be useful for engineering applications by lots of followers, such as (Faltinsen, 1977), (Vinje and Brevig, 1981), (Tanizawa, 1996; Ferrant, 1998; Greco, 2001). Then, 3D Boundary Element Method was developed. (Chahine et al., 1999) modeled the nonlinear evolution of waves progressing along a shallow sloping bottom in the presence of a floating body which is free to rotate and translate. (Bai and Eatock Taylor, 2006) studied the radiation and diffraction problem of vertical circular cylinders in a fully nonlinear numerical wave tank based on the boundary element method (BEM). (You and Faltinsen, 2012) developed a 3D fully nonlinear time-domain Rankine source code.

However, roll motion is closely related with viscous damping. As a result, large errors may be introduced in methods based on potential flow theories by the assumptions that the flow is inviscid and irrotational. To overcome this drawback, a wide variety of nonlinear numerical models based on the N-S equations in time domain have been developed to study the wave-body interaction problem. The Finite Volume method (FVM) combined with interface capturing technique (such as the Level Set method (LS) and the Volume of Fluid method (VOF)) is typically used for spatial discretization. According to the published works of this kind of methods (Boo, 2002; Li, 2010; Ye et al, 2012; Zha et al, 2013; Liu and Wan, 2013), grids are necessary for spatial discretization.

Fortunately, Lagrangian particle methods draw much attention of researchers and are seen as promising numerical approaches for free surface flows. One of them is Moving Particle Semi-implicit (MPS) method, originally proposed by (Koshizuka and Oka, 1996) for incompressible flow. Then, Koshizuka applied MPS into a small body interacting with a breaking wave problem. Compared to grid methods, MPS is a much newer approach and its application about wave-body interaction problem is rarely reported.

In the past works (Zhang et al., 2011a, 2011b, 2011c, 2014; Yang et al., 2014), our in-house improved MPS solver MLParticle-SJTU was applied in many large free-surface deformation problems, such as dam breaking flow, liquid sloshing in LNG tank. The main purpose of the present study is to verify the feasibility of MPS method in solving floating body interacting with waves. Firstly, the improved MPS method for incompressible fluid is described. Numerical approach to solve the motion of floating body is introduced. Then, damped roll motion of a floating box with initial rotational angle is studied to validate effects of water viscosity and spatial resolution of particles. Regular waves are simulated and validated by comparison with analytical results. At last, the roll motion of floating structure in regular waves with difference frequencies is numerically investigated. Response amplitude operators for roll motion are also validated by comparing with experimental results by Jung (2004a).

Numerical Scheme

Original MPS method

The original MPS method is first developed by (Koshizuka, 1996). Its governing equations are the continuum equation and the momentum equation. These equations for incompressible viscous fluid are represented as

$$\nabla \cdot V = 0 \tag{1}$$

$$\frac{DV}{Dt} = -\frac{1}{\rho}\nabla P + \nu\nabla^2 V + g \tag{2}$$

where V is the velocity vector, t is the time, ρ is the density, P is the pressure, ν is the kinematic viscosity, g is the gravity acceleration.

Governing equations are transformed to the equations of particle interactions, and based on the kernel function. In original MPS method, the kernel function is expressed as

$$W(r) = \begin{cases} \dfrac{r_e}{r} - 1 & 0 \le r < r_e \\ 0 & r_e \le r \end{cases} \tag{3}$$

where r is distance between particles and r_e is the effect radius.

The differential operators of gradient, Laplacian and divergence are defined as

$$<\nabla\phi>_i = \frac{d}{n^0}\sum_{j\neq i}\frac{\phi_j - \phi_i}{|\,r_j - r_i\,|^2}(r_j - r_i)\cdot W(|\,r_j - r_i\,|) \tag{4}$$

$$<\nabla^2\phi>_i = \frac{2D}{n^0\lambda}\sum_{j\neq i}(\phi_j - \phi_i)\cdot W(|\,r_j - r_i\,|) \tag{5}$$

$$<\nabla\cdot\mathbf{\Phi}>_i = \frac{d}{n^0}\sum_{j\neq i}\frac{\left(\mathbf{\Phi}_j - \mathbf{\Phi}_i\right)\cdot\left(r_j - r_i\right)}{|\,r_j - r_i\,|^2}W(|\,r_j - r_i\,|) \tag{6}$$

where ϕ is an arbitrary scalar, $\mathbf{\Phi}$ is an arbitrary vector, d is the number of dimensions, n^0 is the initial particle number density for incompressible flow and defined as

$$<n>_i = \sum_{j\neq i}W(|\,r_j - r_i\,|) \tag{7}$$

λ is a parameter, introduced to keep the variance increase equal to that of the analytical solution and defined as

$$\lambda = \frac{\displaystyle\sum_{j\neq i}W(|\,r_j - r_i\,|)\cdot|\,r_j - r_i\,|^2}{\displaystyle\sum_{j\neq i}W(|\,r_j - r_i\,|)} \tag{8}$$

The incompressible condition in original MPS method is represented by keeping the particle number density constant. In each time step, there are two stages: first, temporal velocity of particles is calculated based on viscous and gravitational forces, and particles are moved according to the temporal velocity; second, pressure is implicitly calculated by solving a Poisson equation, and the velocity and position of particles are updated according to the obtained pressure. The Pressure Poisson Equation (PPE) in original MPS method is defined as

$$<\nabla^2 P^{k+1}>_i = -\frac{\rho}{\Delta t^2}\frac{<n^*>_i - n^0}{n^0} \tag{9}$$

where n^* is the particle number density in temporal field.

The free surface boundary conditions, including kinematic and dynamic boundary condition, are imposed on the surface particles. The kinematic condition is directly satisfied in Lagrangian particle method, while the dynamic condition is implemented by setting zero pressure on the free surface particles. So the accuracy of surface particle detection has significant effect on pressure field. The interaction domain is truncated in the free surface (Figure 1), so the particle number density near the

3

free surface is lower than that in the inner field. In original MPS method, particle satisfying (Koshizuka et al., 1998)

$$< n >_i^* \ < \ \beta \, n^0$$ (10)

is considered as free surface particle, where β is a parameter, can be chosen between 0.80 and 0.99.
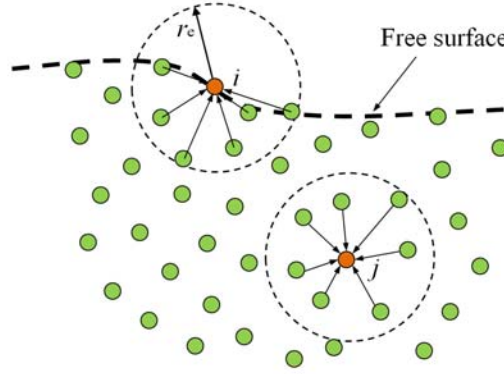

Figure 1 Description of particle interaction domain

Improved MPS method

Compared with original MPS method, four improvements are employed in our in-house solver MLParticle-SJTU, include a new form of kernel function, conservative form of gradient operator, mixed source term for the Poisson equation and a new method for free surface particles detection.

In the present work, we adopt the kernel function suggested by (Zhang and Wan, 2011b), which can be expressed as

$$W(r) = \begin{cases} \dfrac{r_e}{0.85r + 0.15r_e} - 1 & 0 \leq r < r_e \\ 0 & r_e \leq r \end{cases}$$ (11)

The above kernel function has a similar form with the original kernel function Eq. (3), but without singularity.

Original gradient operator as Eq. (4) suffers from a drawback that it cannot conserve the linear and angular momentum of the system. To overcome this, we employ a conservative form as (Tanaka, et al., 2010)

$$< \nabla \phi >_i = \frac{d}{n^0} \sum_{j \neq i} \frac{\phi_j + \phi_i}{|\, \mathbf{r}_j - \mathbf{r}_i \,|^2} (\mathbf{r}_j - \mathbf{r}_i) \cdot W(|\, \mathbf{r}_j - \mathbf{r}_i \,|)$$ (12)

The source term of the Poisson equation in Eq. (9) is solely based on the deviation of the temporal particle number density from the initial value. As the particle number density field is not smooth, the pressure obtained from Eq. (9) is prone to oscillate in spatial and temporal domain. To suppress such unphysical oscillation of pressure, (Tanaka, et al., 2010) proposed a mixed source term for

4

PPE, which combines the velocity divergence and the particle number density. The main part of the mixed source term is the velocity divergence, while the particle number density is used to keep the fluid volume constant. This improved PPE is rewritten by (Lee et al., 2011) as

$$<\nabla^2 P^{k+1}>_i=(1-\gamma)\frac{\rho}{\Delta t}\nabla\cdot V_i^*-\gamma\frac{\rho}{\Delta t^2}\frac{<n^k>_i-n^0}{n^0} \tag{13}$$

where γ is a blending parameter with a value between 0 and 1. The value of γ has large effect on the pressure field. In particular, the larger γ produces smoother pressure field. However, the volume of fluid cannot be constant while $\gamma = 0$. The effects of γ have been investigated by (Tanaka, et al., 2010) and (Lee, et al., 2011), and $\gamma = 0.01$ is used in this paper.

The original detection method (Eq. 10) is based on the particle number density. However, inner particles with small particle number density may be misjudged as free surface particles, thus unreal pressure around the misjudged particles occur. This usually causes nonphysical pressure oscillation. To improve the accuracy of surface particle detection, we employ a new detection method in which a vector function is defined as follow (Zhang and Wan, 2012):

$$<F>_i=\frac{D}{n^0}\sum_{j\neq i}\frac{1}{|r_i-r_j|}(r_i-r_j)W(r_{ij}) \tag{14}$$

The vector function F represents the asymmetry of arrangements of neighbor particles. Particle satisfying

$$<|F|>_i \; > \; \alpha \tag{15}$$

is considered as free surface particle, where α is a parameter, and has a value of 0.9 $|F|^0$ in this paper, $|F|^0$ is the initial value of $|F|$ for surface particle. It should be specially noted that the Eq. (15) is only valid for particles with number density between $0.8n^0$ and $0.97n^0$ since particles with number density lower than $0.8n^0$ is definitely surface particles, while those with number density higher than $0.97n^0$ should get pressure through Poisson equation.

Motion of floating body

The motion of the floating body is governed by the equations of rigid body dynamics, following the Newton's law of motion. The translation motion of the center of gravity and the rotation of the rigid body are given in a simple 2-D framework by

$$\begin{cases} M\dfrac{dV_G}{dt}=Mg+F_{fluid-solid} \\[2mm] I_G\dfrac{d\Omega_G}{dt}=T_{fluid-solid} \end{cases} \tag{16}$$

where M and I_G are the mass and the moment of inertia of the floating body around the center of gravity, respectively. V_G and Ω_G are the linear velocity of the center of gravity and the angular velocity of the body, respectively. $F_{fluid-solid}$ is the hydrodynamic force acting on the body, $T_{fluid-solid}$ is the hydrodynamic torque with the direction normal to the plane.

Numerical Simulations

Validation of hydrostatic pressure

In this section, the improvements employed in our MPS solver MLParticle-SJTU are numerical studied through a simple test of hydrostatic pressure. Figure 2 shows the sketch of calm water tank. The gravitational acceleration and water density are 9.8 m/s^2 and 1000 kg/m^3, respectively. The computational domain is dispersed by particles with initial size of 0.005 m, total number of particles is 9534, and the size of time step is 0.0005.
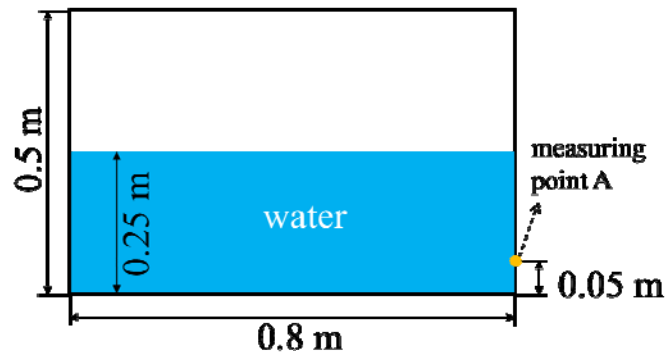

Figure 2 Sketch of calm water tank
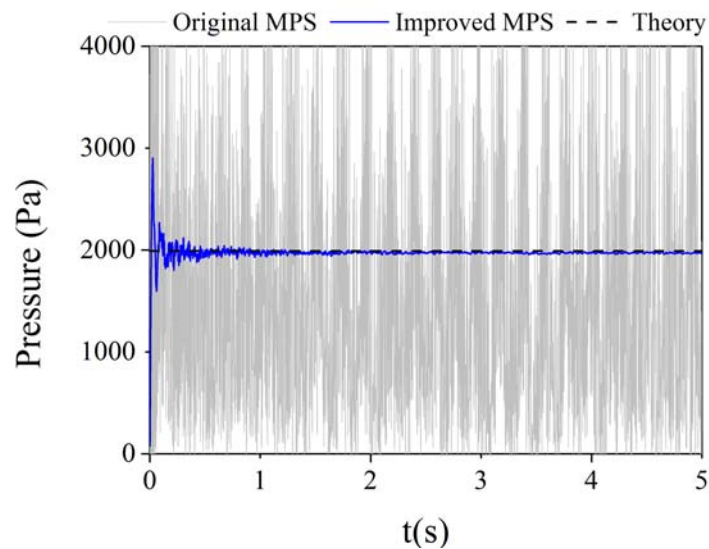
Figure 3 Time history of hydrostatic pressure at measuring point A - Comparison between original MPS and improved MPS method

| (a) original MPS (t = 0.2s) | (b) improved MPS (t = 5.0s) |
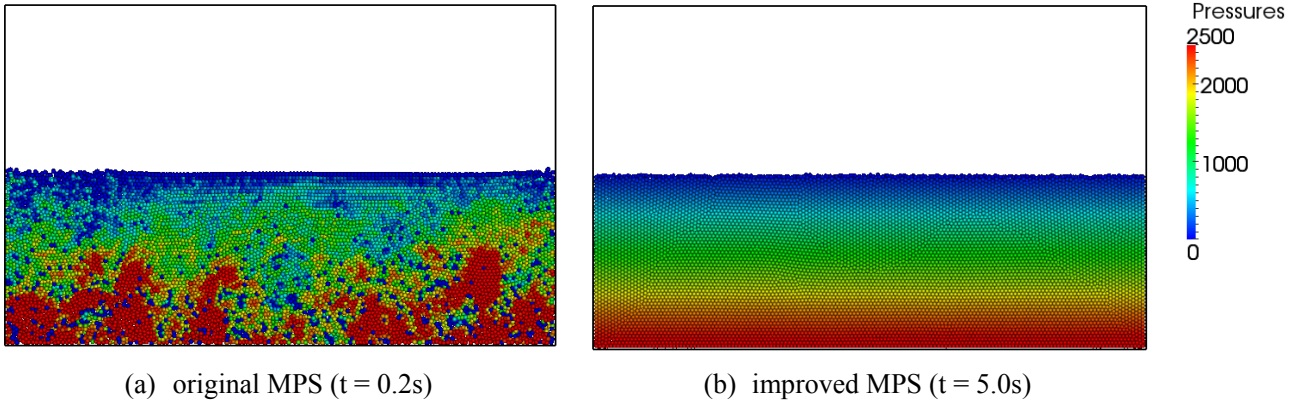
Figure 4 Comparison of hydrostatic pressure fields

Figure 3 shows time variation of hydrostatic pressures at measuring point A, computed by original MPS and improved MPS method. According to the time history curve of pressure calculated by original MPS method, violent unphysical oscillation of pressure occurred in the simulation, amplitudes of pressure fluctuations are significantly different from theoretical value. By contrast, the time history curve of pressure calculated by improved MPS method is much close to theoretical value after about 1.0 s.

Figure 4 shows the comparison of hydrostatic pressure fields between original MPS and improved MPS method. As shown in Figure 5(a), the hydrostatic pressure field at the instant t = 0.2s obtained by original MPS is much rough. Due to the violent oscillation of pressure, fluid field simulated by original MPS is hardly calm down after t = 0.2s. On the other hand, smoothness and regularity of the hydrostatic pressure field shown in Figure 4(b) is significantly enhanced, fluid particles tend to reach an equilibrium state. So, the irregularities of pressure field can be reduced by the improvements proposed in previous section. The improved MPS solver MLParticle-SJTU can be used to simulate realistic pressure field and expected to solve more complex problem.

Validation of damped roll motion

In this section, the damped motion of a floating box is studied to verify the simulation of a floating body with free surface. The initial geometry and set-up are shown in Figure 5. The width and height of the rectangular floating body are 0.3 m and 0.1 m, respectively. The mass moment of inertia of floating body is 0.36 kg·m^2. The box is installed at the symmetrical axis and 0.4 m above the bottom of tank, fixed at the center of its gravity but free in the degree of roll, inclined with the initial angle θ=15°. Density of water is 1000 kg/m^3. Water tank filled with particles of different spatial resolution (0.01 m, 0.004 m, 0.002 m) is simulated to check the convergence of the numerical model.

Since reflex waves generated by the oscillation of box should be avoided to obtain accurate roll angles, sponge layers are placed at both sides of the water tank. In sponge layer, artificial damping term $-\phi(x)V$ is introduced to left hand side of Eq. (2) for absorption of waves and defined as

$$\phi(x) = \begin{cases} 0 & \text{out of sponge layer} \\ \alpha \dfrac{|x - x_0|}{l} & \text{in sponge layer} \end{cases} \tag{17}$$

where α is coefficient for controlling the intensity of the sponge layer, l is width of sponger layer, x_0 is the horizontal position where waves initially enter into the damping layer.
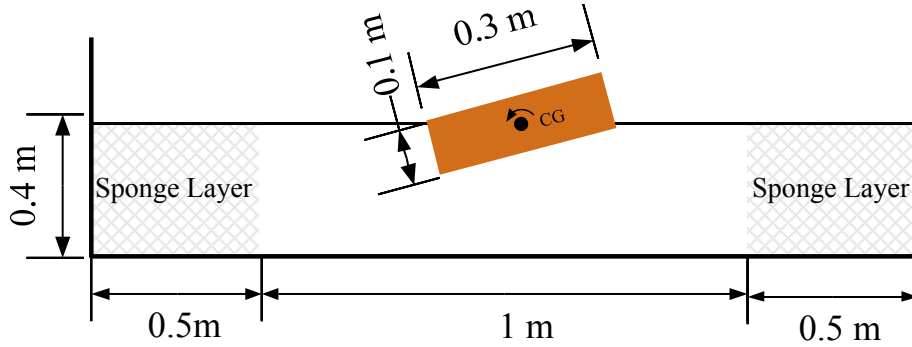
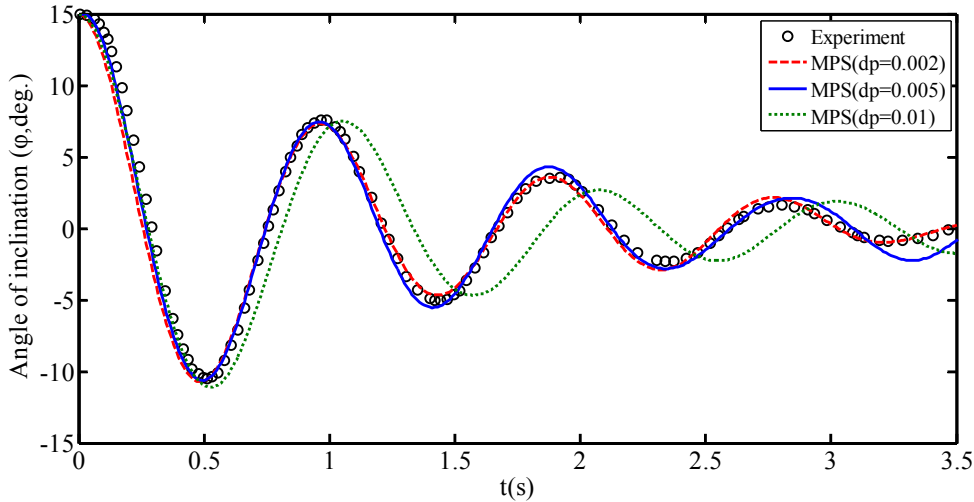

Figure 5 Sketch of damped roll motion

Figure 6 Time history of roll angle during the damped rolling oscillation(dp is the initial distance between particles)

Figure 6 shows the comparison of the time history of roll angles between the computed results with different spatial resolutions and the experimental data. The cycle points represent roll angles obtained by experiment of (Jung, 2004b). The roll motion decays after each period by the damping effect. For the case dp=0.01 m (dp represents distance between particles), period of roll motion is much different from that of experimental data. For the cases dp=0.004 m and dp=0.002 m, both period and amplitude of roll motion agree very well comparing to experimental data. Considering the computational efficiency, initial distance between fluid particles is set to be 0.004 m for all other simulations presented in this paper.

Validation of wave making

In present work, a Numerical Wave Tank (NWT) is developed to study the accuracy of wave making. A piston-type wave generator is incorporated in the left side of 2D NWT. Sponge layer and a slop beach is installed at the end of the wave tank to absorb waves and avoid reflection. Sketch of the numerical setup is shown in Figure 7. The NWT is 5.5 m width and 1.5 m height with initial water depth 0.9 m. Wave conditions used in present numerical test is shown in Table 1, and travelling waves is generated based on linear wave theory.

Table1. Parameters of wave making

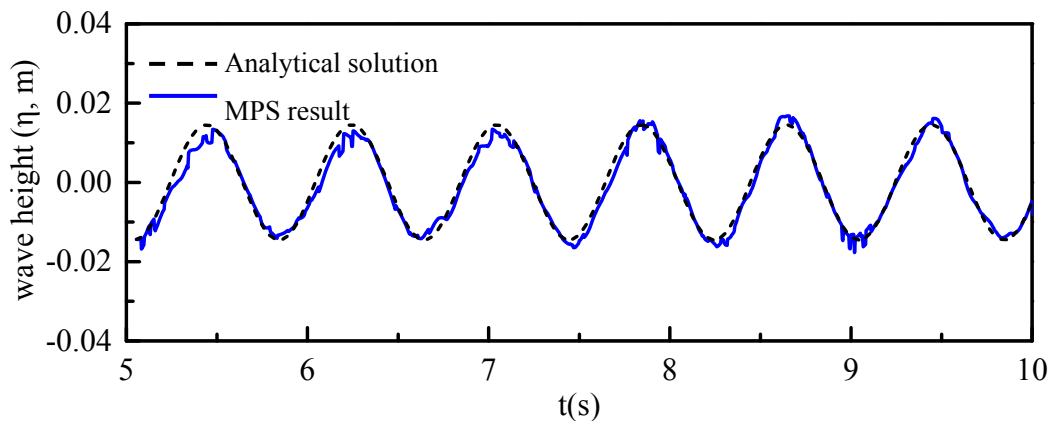| Parameters	Values
Water density(kg/m³)	1000
Water height(m)	0.9
Wave length(m)	1
Wave height(m)	0.029
Wave period(s)	0.8
Fluid spacing(m)	0.004
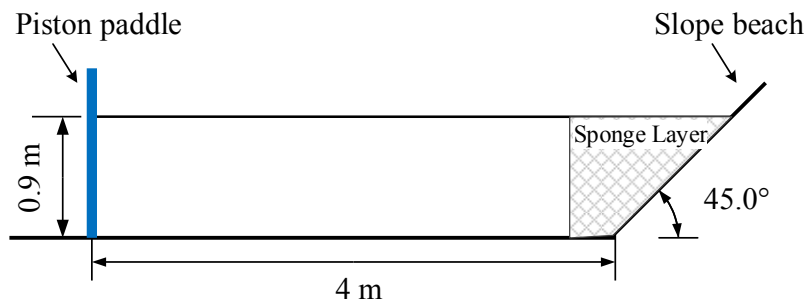
Figure 7 Sketch of the 2-D wave tank

Figure 8 Comparison between numerical wave elevation and analytical solution at location 1.05 m from the piston paddle

9

Figure 8 shows a comparison between numerical wave elevation and analytical solution at the location 1.05 m from the initial position of piston paddle where a floating box will be placed in the next section. The height of free surface simulated by MPS method is in agreement with analytical solution. The difference is that the numerical data is less smoother due to moving of particles at free surface and can be improved by reducing the particle space.

Simulation of floating body freely rolling in waves

In this section, the roll motion of a 2D floating rectangular structure in a NWT is investigated in time domain. The wave generator and wave absorbing manner here are same as that in previous section. The width and height of the rectangular floating body are 0.3 m and 0.1 m, respectively. The structure is installed at the point 1.2 m from the wave maker and 0.9 m above the bottom of tank, fixed at the center of its gravity but free in the degree of roll. The mass moment of inertia of floating body is 0.36 kg·m^2. The natural frequency (ω_N) is 6.78 rad/s, and the natural period (T_N) is 0.93 s for the roll motion. Initial geometry and set-up are shown in Figure 9.
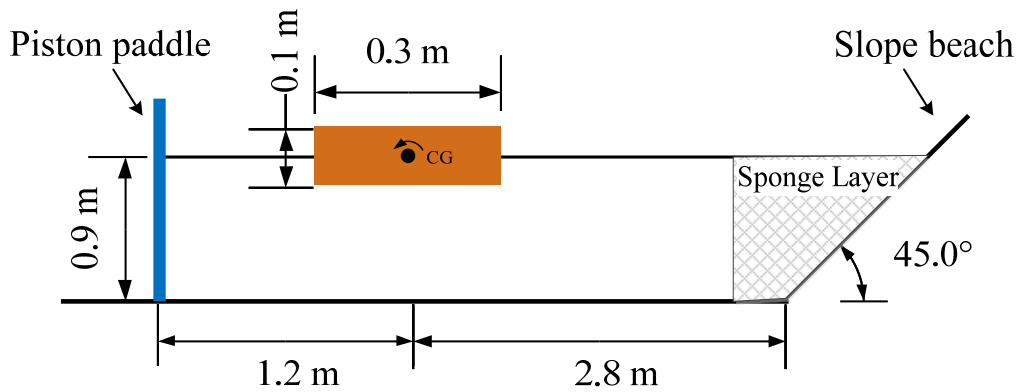

Figure 9 Sketch of the freely rolling body

In present simulation, the distance between particles is 0.004 m. The gravitational acceleration and water density are 9.8m/s^2 and 1000kg/m^3, respectively. The kinematic viscosity of water is given by 1.01×10^{-6} m^2/s. The time step size is 0.0005s and the total computational time is 20s. Cases with different wave periods are investigated in the present study, as shown in Table2.
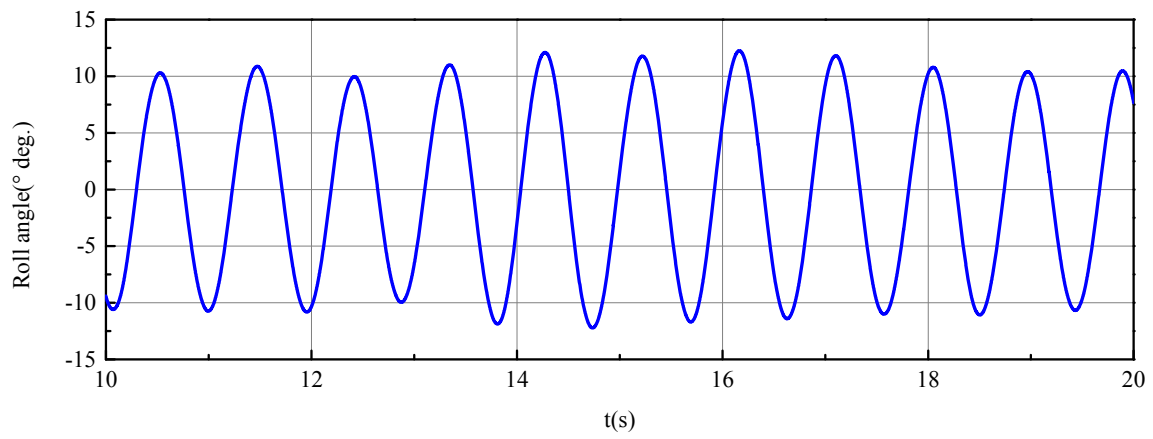
Table2. Parameters of wave making

CASE	T(s)	ω(rad/s)	ω/ω_N	λ(m)	H_I(m)	J(kg·m^2)	$K\zeta_a$
CASE1	0.7	8.98	1.328402	0.77	0.29	0.36	0.1183
CASE2	0.8	7.85	1.161243	1.00	0.29	0.36	0.0911
CASE3	0.93	6.76	1.00	1.35	0.29	0.36	0.0628
CASE4	1.0	6.28	0.928994	1.56	0.29	0.36	0.0584
CASE5	1.2	5.24	0.775148	2.22	0.29	0.36	0.041
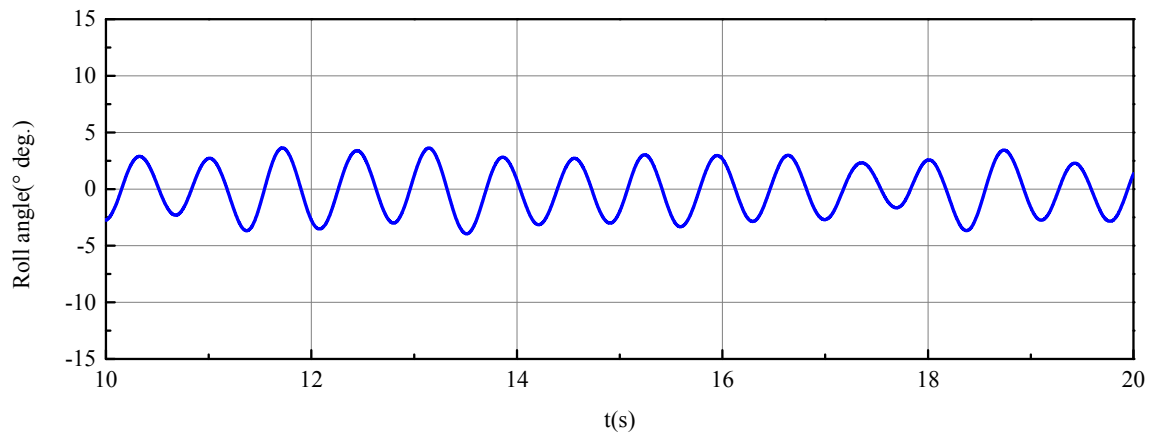
(a) CASE1: ω=8.98rad/s, H$_I$=0.029m
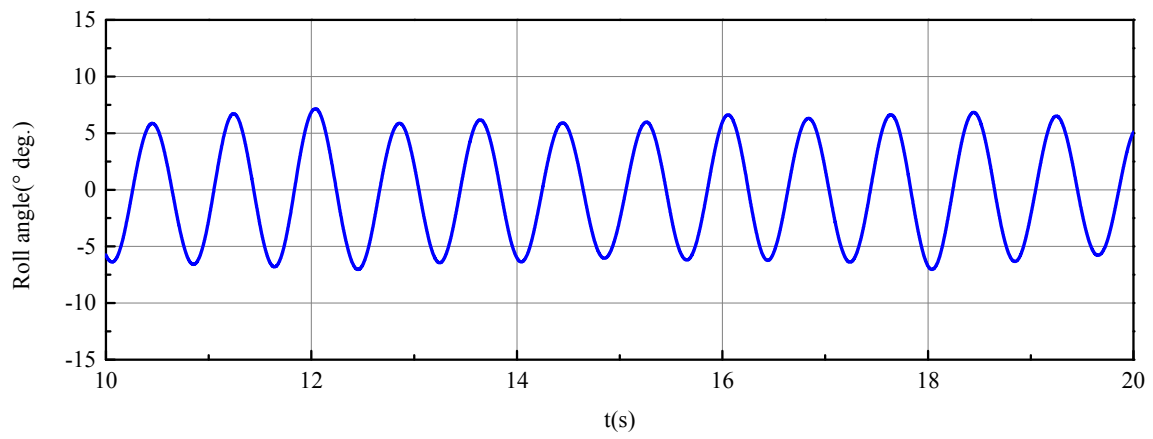
(b) CASE2: ω=7.85rad/s, H$_I$=0.029m

(c) CASE3: ω=6.76rad/s, H$_I$=0.029m
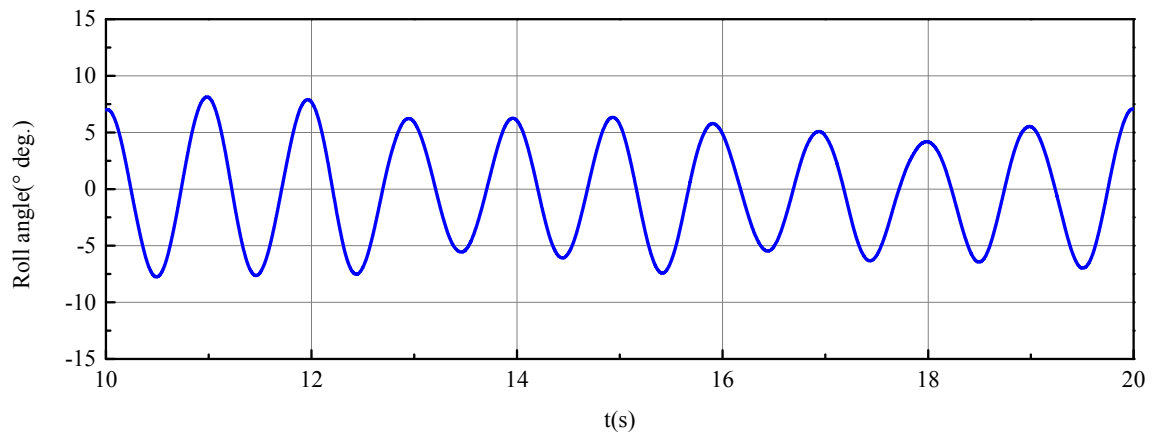
(d) CASE4: ω=6.28rad/s, H$_I$=0.029m
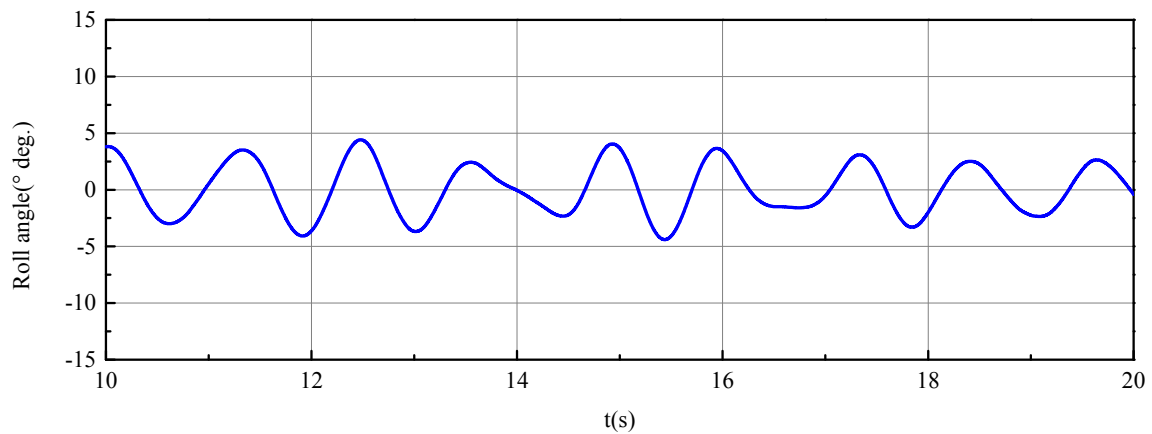
(e) CASE5: ω=5.24rad/s, H$_I$=0.029m

Figure 10 Time history of roll motion, Φ(° deg.)

Figure 10 shows the roll angles of the floating structure for different wave frequencies of ω=8.98rad/s, ω=7.85rad/s, ω=6.76rad/s, ω=6.28rad/s and ω=5.24rad/s. Floating body inclines by the way of simple harmonic motion except the case of ω=5.24rad/s. The maximum amplitude of roll angle is larger than 10 degree, appeared at ω=6.76rad/s where wave frequency is very close to the roll natural frequency of the floating body.
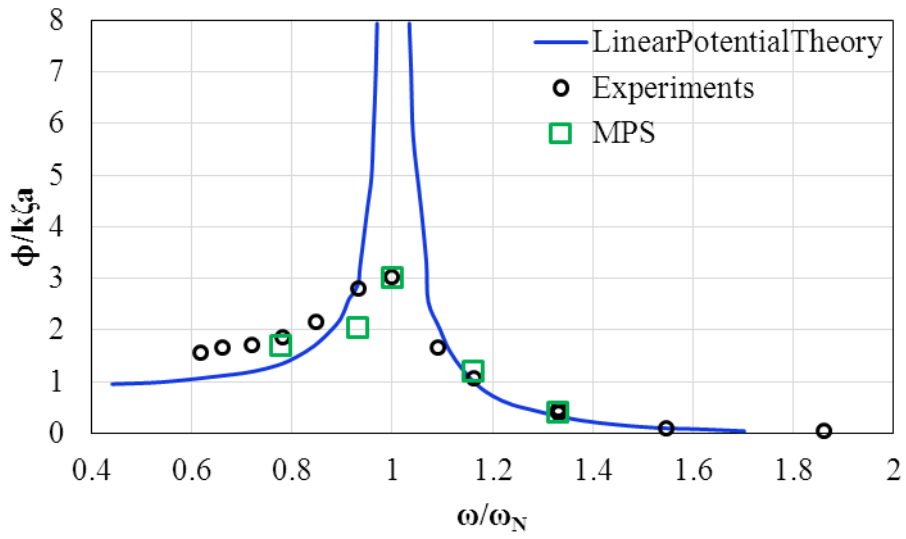
Figure 11 Response amplitude operator (RAO) for roll motion

Figure 11 shows comparison of present RAOs with Jung's experimental results and linear potential theory results as a function of ω/ω_N. ω is the frequency of incident wave and ω_N is the roll natural frequency of the floating body. ϕ and $k\zeta_a$ are the roll angle and the wave slope, respectively. Present RAOs agree well with experimental results, and in good agreements with linear potential theory for higher frequency waves. The roll motion calculated by potential theory is significantly exaggerated at the natural frequency for the ignorance of the viscous damping.
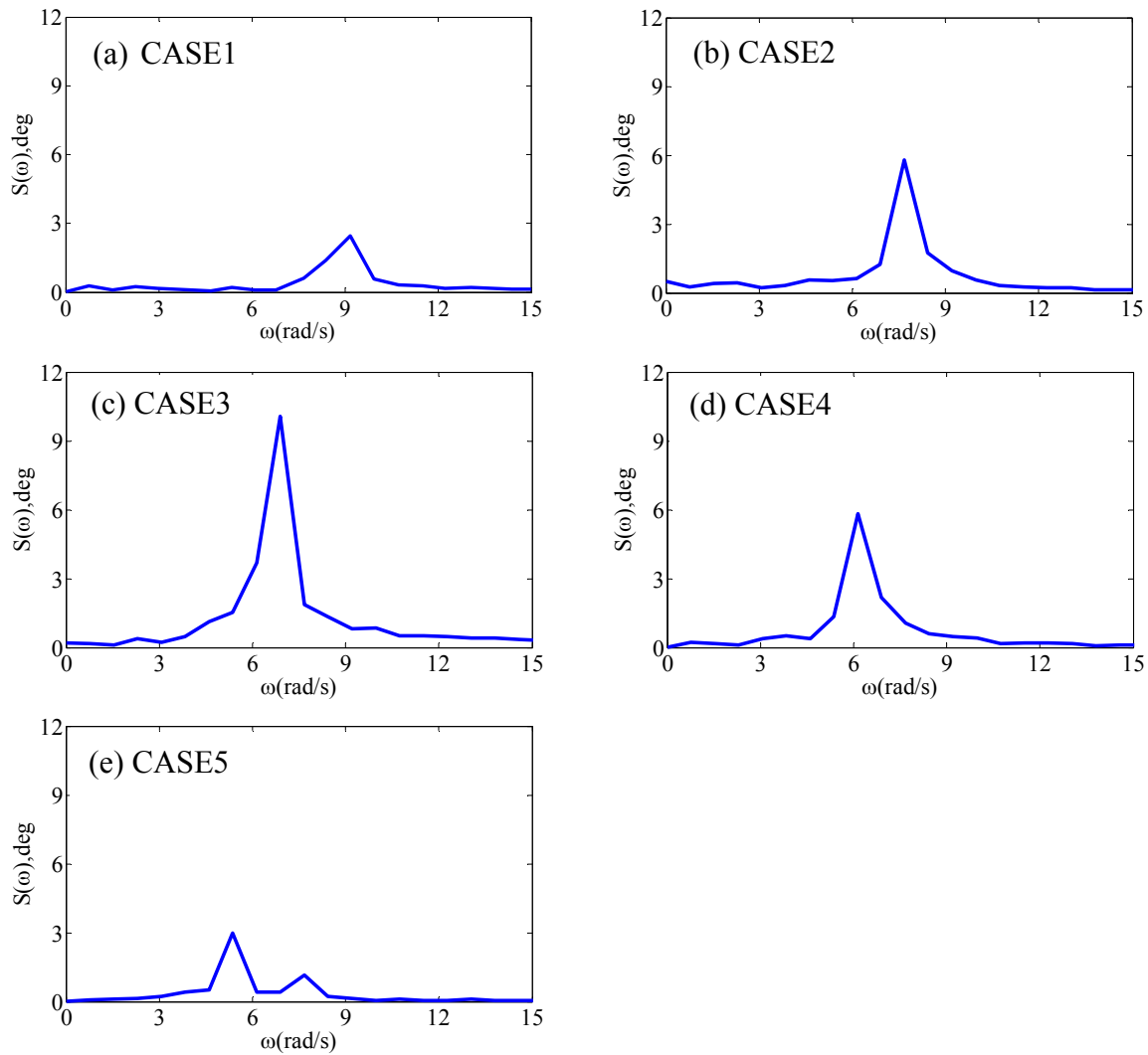
Figure 12 Spectrum of roll motion

As shown in Figure 12, the amplitude spectrums of the roll motions are calculated by Fast Fourier Transformation method. The floating body has the predominant motion at the similar frequency with each incident wave (ω = 8.98rad/s, 7.85 rad/s, 6.76 rad/s and 6.28rad/s). At the incident wave frequency of 5.24 rad/s, the roll motion of double frequency was present.

Conclusions

In this paper, interaction between regular waves and free roll motion of a 2D floating body is investigated by our in-house particle solver MLParticle-SJTU based on improved Moving Particle Semi-Implicit (MPS) method. The comparison between the numerical wave elevation and the analytical solution shows that the MLParticle-SJTU can produce waves with acceptable accuracy. Time histories of roll angles of the floating structure for five different wave frequencies are presented, the maximum amplitude of roll angle appeared while wave frequency was very close to the natural frequency of the floating body. Response amplitude operators (RAO) for roll motions agree well with Jung's experimental results. Furthermore, it's shown that frequencies of roll

14

motions are similar with those of incident waves. According to the results present in previous sections, the MPS solver can be used to deal with waves floating body interaction problems.

Acknowledgement

References

Bai, W., and Taylor, R. E. (2008) Fully nonlinear simulation of wave interaction with fixed and floating flared structures. *Ocean Engineering*, 36(3), 223-236.

Boo, S.Y., (2002) Linear and nonlinear irregular waves and forces in a numerical wave tank. *Ocean Engineering*, 29, 475-493.

Faltinsen, O. M. (1977) *Numerical solutions of transient nonlinear free-surface motion outside or inside moving bodies*. Proceedings of the Second International Conference on Numerical Ship Hydrodynamics, University of California, Berkeley, Extension Publications, 347-357.

Ferrant, P. (1998) *Fully nonlinear interactions of long-crested wave packets with a three dimensional body*. Proceedings of the 22nd International Conference on Numerical Ship Hydrodynamics, Washington, DC, 403-415.

Greco, M. (2001) *A Two-Dimensional Study of Green-Water Loading*. Norwegian University of Science and Technology, Department of Marine Hydrodynamics, NTNU, Trondheim, Norway.

Jung, K.H., Chang, K. A. and Huang, E.T. (2004a) Two-dimensional flow characteristics of wave interactions with a fixed rectangular structure. *Ocean Engineering*, 31, 975-998.

Jung, K. H. (2004b) Experimental study on rectangular barge in beam sea, Ph.D. Texas A&M University.

Jung, K. H., Chang, K. A. and Huang, E.T. (2005) Two-dimensional flow characteristics of wave interactions with a free-rolling rectangular structure. *Ocean Engineering*, 32(1), 1-20.

Kalumuck, K. M., Chahine, G. L., and Goumilevski, A. G. (1999) *BEM modeling of the interaction between breaking waves and a floating body in the surf zone*. 13th ASCE Engineering Mechanics, Baltimore, Maryland.

Koshizuka, S., and Oka, Y. (1996) Moving-particle Semi-implicit Method for Fragmentation of Incompressible Fluid. *Nuclear Science and Engineering*, 123, 421-434.

Koshizuka, S., Obe, A., and Oka, Y. (1998) Numerical Analysis of Breaking Waves Using the Moving Particle Semi-implicit Method. *International Journal for Numerical Methods in Fluids*, 26, 751-769.

Koshizuka, S., Shibata, K., Tanaka, M. Suzuki, Y. (2007) *Numerical analysis of fluid-structure and fluid-rigid body interactions using a particle method*. Proceedings of FEDSM, San Diego, California, USA, 2007-37137.

Lee, B. H., Park, J. C., Kim, M. H. and Hwang, S. C. (2011) Step-by-step improvement of MPS method in simulating violent free-surface motions and impact-loads. *Computer Methods in Applied Mechanics and Engineering*, 200:1113-1125.

Li, Y., and Lin, M. (2010) Wave-body interactions for a surface-piercing body in water of finite depth. *Journal of hydrodynamics, Ser. B*, 22 (6), 745-752.

Liu, Y. C., and Wan, D. C. (2013) *Calculation of motion response for moored floating pier in waves*. Proc 25rd Chinese National Conf Hydrodynamics, ZhouShan, China.

Longuet, M. S., Cokelet, C. D. (1976) *The deformation of steep surface waves on water, a numerical method of computation*. Proceedings of the Royal Society of London A350, 1-26.

Ren, B., He, M., Dong, P., and Wen, H. J. (2015) Nonlinear simulations of wave-induced motions of a freely floating body using WCSPH method. *Applied Ocean Research*, 50 (2015) 1-12.

Shibata, K., Koshizuka , S., Sakai, M., Tanizawa, K., and Ota, S. (2011) *Numerical Analysis of Acceleration of a Free-fall Lifeboat Using the MPS Method*. Proceedings of the Twenty-first International Offshore and Polar Engineering Conference, Maui, Hawaii, USA, 19-24.

Tanaka, M., and Masunaga, T. (2010) Stabilization and smoothing of pressure in MPS method by Quasi-Compressibility. *J Comp Phys*, 229, 4279-4290.

Tanizawa K. (1996) *Nonlinear simulation of floating body motions in waves*. The proceedings of the 6th international offshore and polar engineering conference, vol III. ISOPE, Golden, CO, USA, 414-420.

Vinje, T., Brevig, P. (1981) *Nonlinear ship motions*. Proceedings of the Third International Conference on Numerical Ship Hydrodynamics, Paris, France, 1-10.

Yang, Y. Q., Zhang, Y. X., Tang, Z. Y., and Wan, D. C. (2014) *Numerical study on liquid sloshing in horizontal baffled tank by MPS method*. Proc 26rd Chinese National Conf Hydrodynamics, QingDao, China.

You, J., Faltinsen, and O. M. (2012) *A 3D Fully Nonlinear Numerical Wave Tank with a Moored Floating Body in Shallow Water*. Proceedings of the Twenty-second International Offshore and Polar Engineering Conference Rhodes, Greece.

Ye, H. X., Shen, Z. R., and Wan, D. C. (2012) *Numerical analysis of large amplitude motion responses for a container ship in waves*. Proc 24rd Chinese National Conf Hydrodynamics, Wuxi, China.

Zha, R, S, Ye, H. X., and Wan, D. C. (2013) *Numerical investigation of ship sea-keeping performances in head regular waves*. Proc 25rd Chinese National Conf Hydrodynamics, ZhouShan, China.

Zhang, Y. X., and Wan, D. C. (2011a) *Application of Improved MPS Method in Sloshing Problem*. Proc 23rd Chinese National Conf Hydrodynamics, Xi'an, China.

Zhang, Y. X., and Wan, D. C. (2011b) *Apply MPS Method to Simulate Motion of Floating Body Interacting with Solitary Wave*. Proc 7th Int Workshop Ship Hydrodynamics, IWSH, Shanghai, China, 275-279.

Zhang, Y. X., and Wan, D. C. (2011c) Application of MPS in 3D Dam Breaking Flows. *Sci Sin Phys Mech Astron*, 41, 140-154.

Zhang, Y. X. and Wan, D. C. (2012) Numerical Simulation of Liquid Sloshing in Low-Filling Tank by MPS. *Journal of Hydrodynamics*, 27:100-107.

Zhang, Y. X., Wan, D. C., Hino, and Takanori. (2014) Comparative study of MPS method and level-set method for sloshing flows. *Journal of hydrodynamics*, 26(4), 577-585.